Journal of Network Intelligence
Taiwan Ubiquitous Information
 ISSN 2414-8105 (Online)
Volume **7**, Number **3**, August **2022**

Image Splicing Detection Based on Complex Features of Camera Noise Characteristics

Yi-Jia Zhang, Tong-Tong Shi

School of Information Science and Technology
Zhejiang Sci-Tech University
Hangzhou 310018, P. R. China
waiting@zstu.edu.cn

Zhe-Ming Lu*

School of Aeronautics and Astronautics
Zhejiang University
No. 38, Zheda Road, Hangzhou 310027, P. R. China
zheminglu@zju.edu.cn

*Corresponding author: Zhe-Ming Lu

Received July 23, 2021, revised September 17, 2021, accepted January 30, 2022.

Abstract. *The image captured by the camera has different camera noise compared to the splicing image. First, the splicing image and the original image are inconsistent in internal statistical characteristics. Secondly, the image splicing affects the image content, resulting in inconsistent texture information. Most importantly, the difference in the source of the pictures leads to inconsistencies between the splicing image and the original image due to camera noise. These inconsistencies in characteristics can be used as a means of image splicing detection. Therefore, this paper combines the advantages of the three methods and proposes a method for tampering detection of composite image splicing based on the three features of camera, texture and statistics. The first step is to extract the statistical features of the gray-level histogram and gray-level co-occurrence matrix of the image. The second step is to extract the LBP of the grayscale image as the texture feature. Third, we adopt the wavelet filtering-based light response non-uniform noise (PRNU) as image features, and then extract PRNU statistical information and texture features as noise features. Finally, we adopt the SVM method for classification. Experimental demonstrate the effectiveness of the proposed scheme.*
Keywords: Image splicing tampering detection, inconsistencies, camera noises, PRNU, composite features

1. **Introduction.** With the rapid development of information technology and smart devices, digital images have promoted the efficiency of information transmission with their intuitiveness and timeliness. Nowadays, almost everyone can perform various tampering operations on pictures through image editing software. Many people use images for deliberate modification and careful forgery, and the traces of tampering are difficult to identify with the naked eye. What's more, the images are tampered with for ulterior purposes and maliciously spread and spread. If these falsified digital images are inappropriately used in important fields, such as news, military, medicine, and scientific research, it will cause immeasurable harm to national politics and people's lives. Therefore, it is very important to ensure the integrity and authenticity of the digital image source. Digital image forensics is an effective means of detecting tampering, and image splicing detection

is one of the research hotspots in the field of passive forensics. Image splicing is a basic and widely used method of tampering. It is a technique for cutting and pasting image areas from the same or different images. Because image splicing detection is an important and challenging research field, this article mainly studies digital image splicing detection.

Pictures taken by a digital camera will inevitably bring noise inside the camera, which is consistent. The splicing operation between different images will also produce noise discontinuity. Camera noise is an inherent characteristic of the camera, which is difficult to remove for tampering operations. Therefore, camera noise can be used as a basis for judging the authenticity of an image. In 2006, Lukas et al.[1] first proposed the use of Photo-Response Non-Uniformity (PRNU) for image tampering detection. In 2009, Goljan et al. [2] used maximum likelihood estimation to extract fingerprints from digital cameras, remove non-unique artifacts from fingerprints, extract noise residues from images, and calculate peak correlation ratio correlation verification. After continuous experimental research [3-8], it has been confirmed that the light response non-uniformity can be used as the only fingerprint of a digital camera. In 2010, Chierchia et al. [9] confirmed that denoising is effective for splicing detection using PRNU. After three years, they proposed a Bayesian classification method in [10], which used the minimum risk assessment, mainly to minimize the error probability and obtain better detection results. According to the fact that images from different sources have different amounts of noise, Pan et al. [11] described an effective method for exposing image splicing by detecting inconsistent local noise variances. In 2016, Pun et al. [12] proposed a multi-scale noise difference method to detect image splicing, which divides the image into multiple proportions of super-pixel blocks. There are also some fusion schemes of multiple algorithms to achieve better results. For example, Cozzolino et al. [13] used camera noise, machine learning, and block matching to perform image tampering detection, and the detection rate on IEEE IFS-TC was 40.72%. In 2015, Gaborini et al. [14] also proposed a fusion image tampering detection algorithm based on three independent algorithms: PRNU, image system analysis, and block matching, which has the best effect on IEEE IFS-TC. In 2019, Reference [15] proposed a method based on the non-uniformity of light response (PRNU) and a method based on the statistical characteristics of the Dempster-Shafer theory. In 2020, Reference [16] used super-pixel algorithm to perform non-overlapping segmentation of detected images, and calculate the correlation of PRNU on super pixel to determine whether there is tampering. Reference [17] used image segmentation and multi-directional detection window to obtain the forgery probability. Recently, the combination of deep learning and camera noise [18] for image tampering detection has also achieved good results. Of course, image processing and detection are not only used in image forensics. In recent years, image detection has shown great advantages in medical image segmentation [19], road target recognition [20], and traffic pattern detection [21], which are closely related to our lives as forensics.

Even though there are many image tamper detection techniques available in the current literature, further improvements in accuracy is needed for reliable forgery detection. In this paper, we propose a detection algorithm of composite feature image splicing based on camera noise. In order to study the feature inconsistency between the original image and the splicing image, this paper analyzes the inconsistency of the original image and the splicing image on three features, i.e., camera, texture and statistics, and proposes a low-dimensional composite feature image splicing detection method. First, we extract the statistical features of the gray histogram and gray co-occurrence matrix on the gray image; then, we extract the local binary pattern as texture features; finally, we extract the PRNU statistical information and texture features as noise features. The experimental

results of the paper show that our method can effectively detect image splicing, and the accuracy on the Columbia splicing dataset is 97.35%.

The rest of the paper is organized as follows. Section 1 reports the related works. Section 2 explains our proposed method in detail. Section 3 discusses the experimental result of our proposed method. Finally, Section 4 concludes the whole paper.

2. **Proposed methodology.** The existing image tampering detection algorithm based on camera noise uses camera reference noise as fingerprint recognition, and then extracts the residual image noise from a single image, and cross-correlates it with the camera reference pattern noise for image tampering detection. Although this algorithm can obtain high detection performance for various tampering operations (such as image copy, paste and splicing), its computational complexity is too high. This paper mainly proposes an image splicing tampering detection method based on the composite features of camera, texture and statistics. The detection is based on the inconsistency of statistics, texture and noise characteristics of natural images and tampered images. The first step is to extract the mean, variance, skewness, peak and median of the gray-level histogram, and extract the three statistics features of the gray level co-occurrence matrix (GLCM) of the image, contrast and entropy at the same time. The second step is to extract the LBP of the grayscale image as the texture feature. Third, we adopt wavelet filtering-based light response non-uniform noise (PRNU) as initial features, and then extract PRNU statistical information and texture features as noise features. Finally, we adopt SVM for classification.

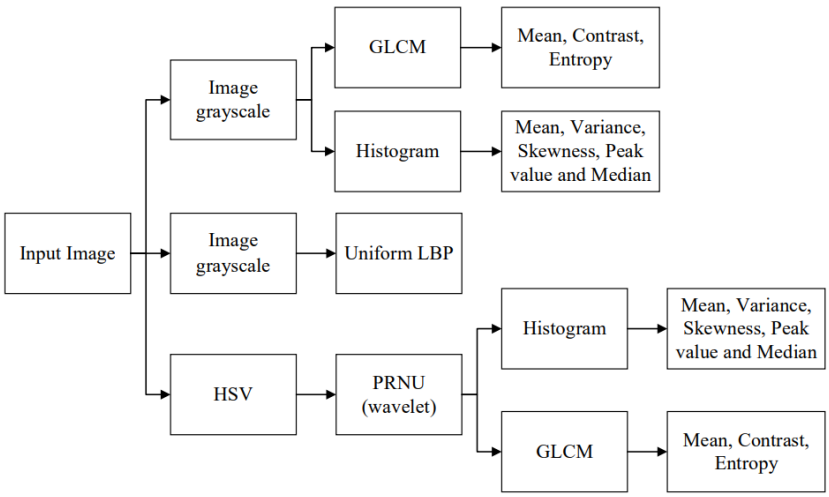

FIGURE 1. Framework of the proposed scheme

2.1. **Feature Extraction.** In this subsection, based on the difference among statistics, texture and noise features, a feature extraction method for image splicing detection is provided, as shown in Fig. 1. In terms of statistical features, we extract the statistics of the gray histogram and gray level co-occurrence matrix, a total of 8-dimensional features; in terms of texture features, we extract uniform local binary patterns, a total of 59-dimensional features; in terms of pattern noise, we extract the statistical information of the noise in the three color channel modes of HSV as the noise feature, totally 24 dimensions. The detailed process is as follows:

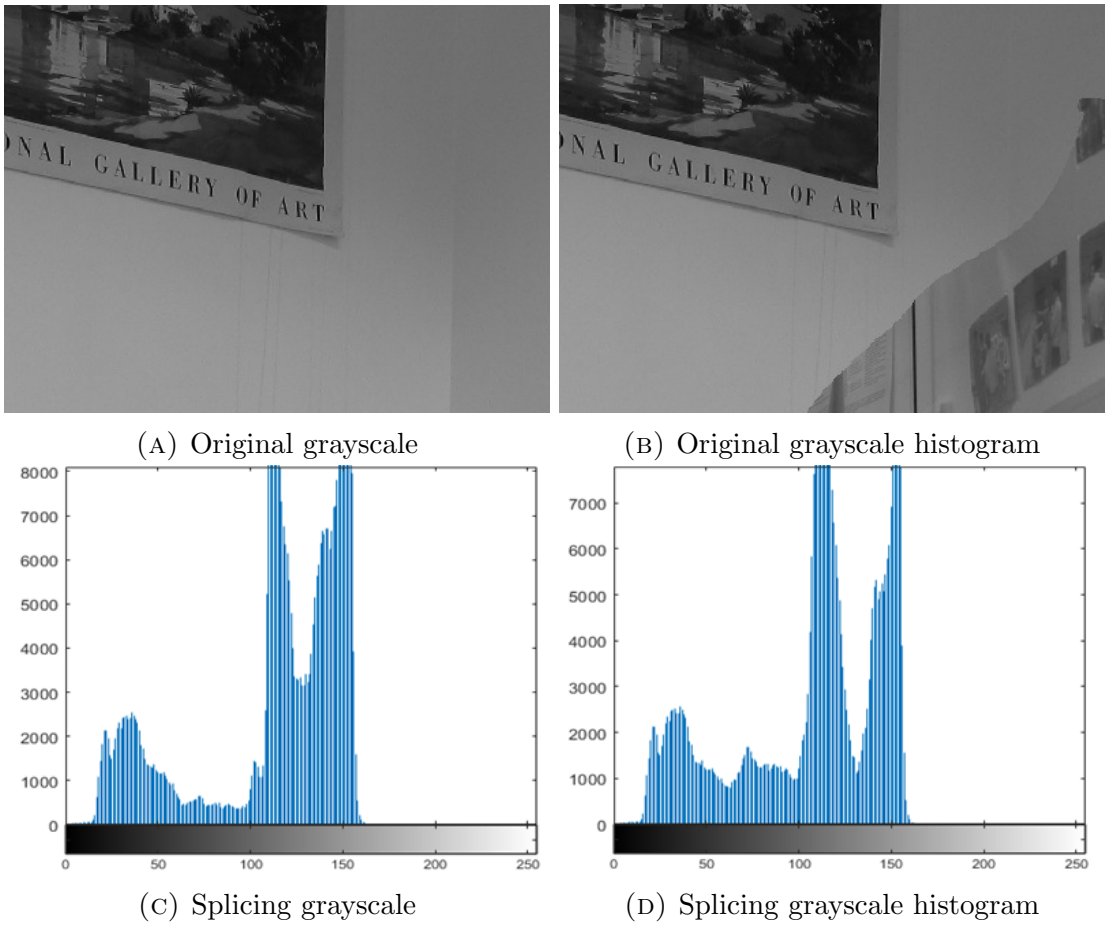

(A) Original grayscale (B) Original grayscale histogram

(C) Splicing grayscale (D) Splicing grayscale histogram

FIGURE 2. Two types of image grayscale histogram.

2.1.1. *Statistical Feature.* Since the splicing operation will cause changes in the internal statistical characteristics of the image, and the grayscale histogram of the image contains most of the statistical information of the image. Figure 2 shows that the grayscale histograms of the original image and the splicing image have obvious distribution inconsistencies, so the gray histogram is selected for feature extraction. Many previous algorithms used histograms of RGB channels to extract features, but in order to reduce the dimensionality of features, gray-scale image histograms are used. Secondly, three statistics features of the gray-level co-occurrence matrix are also extracted. This paper only selects the three variables of average, contrast and entropy as features.

The calculation formula of the gray level co-occurrence matrix is shown below.

Mean (MEAN): The mean value reflects the regularity of the texture. The messy texture is difficult to describe and the value is small; the regularity is easy to describe and the value is large.

$$MEAN = \sum_{a} a \sum_{b} \delta_{\phi,d}(a,b) \tag{1}$$

where a and b mean the rows and columns of the elements of the gray level co-occurrence matrix, ϕ means the direction, d means the distance, and $\delta_{\phi,d}(a,b)$ means the joint distribution of the two pixels with spatial positional relationship.

Contrast (CON): The contrast reflects the degree of change of the gray level of the partial image. The greater the difference between gray levels in the image, the sharper

the edge of the image, and the greater the contrast.

$$CON = |a-b|^k \delta^{\lambda}_{\phi,d}(a,b) \tag{2}$$

where k is often set to be 2, λ is often set to be 1.

Entropy (ENT): It is a measure of the amount of information in the target image. Texture information is also an aspect of entropy measurement. The elements in the image are more dispersed, the greater the entropy, and the smaller the conversely. The size of the entropy represents the uniformity or complexity of the target image texture.

$$ENT = \sum_{a,b} \delta_{\phi,d}(a,b) \log_2 \delta^{\lambda}_{\phi,d}(a,b) \tag{3}$$

2.1.2. *Texture Feature.* The texture information and color information of the image do not have a great influence on each other, therefore, only grayscale images are used to extract texture features. The texture information of some areas of the image is richer, while some parts are relatively flat, and the flat parts contain less texture information. LBP is an abbreviation of Local Binary Pattern, which has significant advantages such as gray scale invariance and rotation invariance. Because of its simplicity and ease of calculation, this feature has been widely used. The LBP operator can be expressed by Eq. (5).

$$LBP_{P,R}(x_c, y_c) \sum_{i=0}^{P-1} 2^i s(g_i - g_c) \tag{4}$$

where P is the number of surrounding points and R means the radius of the center pixel, in our method, we set $R = 1$, $P = 8$. (x_c, y_c) denotes the center pixel, g_c is its gray value, g_i stands for the gray value of its adjacent pixel, and s is a sign function defined as follows.

$$s(x) = \begin{cases} 1 & x \geq 0 \\ 0 & x < 0 \end{cases} \tag{5}$$

We use the histogram statistics of the LBP features, that is, the statistics of the proportions of the LBP features among 0 to 255, so that the dimensionality reduction of the data is performed. That is, reclassify the original 256-dimensional grayscale data and count the number of transitions after displacement. When the number of transitions is less than 2 times, it is defined as a Uniform LBP. After statistics, Uniform LBP accounts for 85%∼90% of the entire LBP features, while has only a dimension of 58. That is, we can reduce the classification feature vector from dimension 256 to dimension 58. In practical applications, the vector is 59 dimensional, because adding one dimension represents those quantities that are not Uniform LBP. For the input image, the grayscale preprocessing is performed first, and after the grayscale images of the two types of images are obtained, the original image and the splicing image are respectively extracted with uniform mode LBP features, and 59-dimensional features are obtained here. Take these 59-dimensional features as texture features.

2.1.3. *Camera Noise Feature.* Camera noise is closely related to pixel value, so the three channels of HSV will all have an impact on camera noise, so it needs to be calculated separately. First, the color space conversion from RGB to HSV is performed to obtain three-channel images, and subsequent feature extraction is performed on the three-channel images.

Camera noise is a kind of multiplicative noise and highly correlated with pixel value, it is very difficult to get through accurate calculation. In the existing methods, for the calculation of the camera mode noise, wavelet filtering is mostly used to calculate the mode noise for all images, and then the average value is obtained as the camera's reference

mode noise. Finally, the correlation between the pattern noise of the image under test and the reference pattern noise of the device is used to identify the noise source. However, this amount of calculation is unbearable. Therefore, this paper does not perform a large number of calculations on the reference pattern noise, but focuses on the study of how to extract the features of the camera noise.

Obtaining the noise residuals containing PRNU components in the image is the key to feature extraction. Therefore, this paper adopts the low-pass filter extraction method based on wavelet filtering. The specific steps are as follows:

1. Using the "db8" four-level wavelet decomposition for the three channels of the image respectively, the sub-bands in the diagonal, horizontal and vertical directions of each level of decomposition can be obtained;

2. For each sub-band, a sliding window is used on each wavelet coefficient. In addition, the maximum a posteriori estimation method is used to estimate the local variance of each wavelet. Take the sub-band as an example:

$$\hat{\delta}_w^2(i,j) = \max\left(0, \left(\frac{1}{w^2}, \sum_{(i,j)\in N} h^2(i,j)\right) - \delta_0^2\right), (i,j) \in J \tag{6}$$

Among them, J is the size of the sub-band, $h(i,j)$ is the value of a certain horizontal sub-band component at (i,j), and the maximum value of $\max(\cdot)$ is obtained. Select the minimum value in the neighborhood window as the final estimate:

$$\hat{\delta}^2(i,j) = \min\left(\hat{\delta}_3^2(i,j), \hat{\delta}_5^2(i,j), \hat{\delta}_7^2(i,j), \hat{\delta}_9^2(i,j)\right), (i,j) \in J \tag{7}$$

Among them, $\min(\cdot)$ is to obtain the minimum value.

3. The wavelet coefficient values after denoising are obtained by Wiener filter:

$$h_{dem}(i,j) = h(i,j)\frac{\hat{\delta}^2(i,j)}{\hat{\delta}^2(i,j) + \delta_0^2} \tag{8}$$

4. The denoising image is finally obtained by inverse wavelet transform. As shown in Figure 3.

FIGURE 3. Extraction method based on wavelet filtering

2.2. **Classification.** We use the SVM to classify the pictures. In order to obtain a reliable and stable model, the ten-fold crossover method is used for verification.

Repeat the above steps for the real images and splicing images in the data set, extract the above three classification features, and then perform training and testing. This article is a classic binary classification problem. Therefore, this article marks the original image as 0 and the tampered image as 1. Then, the detailed steps of the algorithm for image splicing and tampering detection and identification are as follows:

(1) Prepare the data set. Randomly select the original image and the spliced tampered image from the data set as the training image; the remaining images are used as the test group image, and the ratio of the training set to the test set is 8:2;

(2) Training. The three types of features extracted from the training group are weighted and then sent to the classifier and subjected to 10-fold cross-validation to obtain the SVM model;

(3) Forecast. Extract the composite features of the test set, and then send it to the classifier, use the trained SVM model to test, and finally get the recognition accuracy of the algorithm.

In our paper, 10-fold cross-validation, used to test algorithm accuracy. It is a commonly used test method. Divide the data set into ten sub-sets, taking 9 of them as training data and 1 as test data in turn. Each test will give the corresponding correct rate (or error rate). The average value of the accuracy rate (or error rate) of the results of 10 times is used as an estimate of the accuracy of the algorithm.

3. **Experimental Results and Discussions.** This section begins with the introduction of datasets, followed by the evaluation of our proposed algorithm, and we compare the method with a single algorithm. All the experiments are conducted on a desktop equipped with Core-i7 and 8-GB RAM, and the implementation and the experimentation of the algorithms were carried out using MATLAB® R2020a version.

3.1. **Datasets.** We chose three public datasets for evaluation, i.e., COLUMB, MICC-F220, MICC-F2000, CASIA 2.0 are used to demonstrate the effectiveness of our scheme. More details can be found below.

Table 1. Datasets

Dataset	Real	Tamper	Resolution	Post-processing
COLUMB	183	180	$757 \times 568 - 1152 \times 768$	None
MICC-F220	110	110	$722 \times 480 - 800 \times 600$	Rotate, Zoom
MICC-2000	1300	700	2048×1536	Rotate, Zoom
CASIA 2.0	7491	5123	$240 \times 160 - 900 \times 600$	Rotate, zoom, blur

3.2. **Evaluation.** To evaluate the performance of tampering detection, we use the *Precision* and *Recall* which are respectively defined in Eq. (9) and Eq. (10). The *Precision* means the probability that the detected regions are relevant, and it is defined as the ratio of number of correctly detected forged pixels to the number of totally detected forged pixels; while the *Recall* means the probability that the relevant regions are detected, and it is defined as the ratio of number of correctly detected forged pixels to the number of forged pixels in the ground-truth forged image.

$$Precision = \frac{TP}{TP + FP} \tag{9}$$

$$Recall = \frac{TP}{TP + FN} \tag{10}$$

Where TP denotes the tampered region correctly detected as tampered; FP denotes the non-tampered region incorrectly detected as tampered; and FN denotes tampered region incorrectly detected as non-tampered. Therefore, $TP + FP$ means the total detected region, and $TP + FN$ means the real tampered region, that is the ground-truth result for

judgment. In addition to the *Precision* and *Recall*, we calculate the F_1 score using Eq. (11), to synthesize the Precision and Recall as a new evaluating indicator.

$$F_1 = \frac{2 \times Precision \times Recall}{Precision + Recall} \tag{11}$$

3.3. **Discussion.** In this section, the experimental results of this paper will be analyzed in detail. Because this paper adopts the design fusion of multiple features, the statistical features, texture features, camera noise features, and composite features are evaluated separately, and the evaluation indicators are still used. The precision rate, recall rate, F1 evaluation index and accuracy rate mentioned in the paper, each index is shown in the table below. This article evaluates and compares single and compound features.

TABLE 2. Performance evaluation of different methods

Feature	Precision (%)	Recall (%)	F1 score(%)	Accuracy (%)
Statistical	80.11	82.78	81.42	87.14
Texture	87.21	83.33	85.23	90.17
Camera noise	87.43	92.78	90.03	93.00
Complex feature	**94.15**	**98.33**	**96.19**	**97.35**

From Table. 2, we can see that each single feature has its own advantages, and our feature fusion is to combine the advantages. Therefore, in order to select the best features and make up for the shortcomings of some features, this paper combines the three features to improve the accuracy of classification. It can be concluded from the above table that the performance of a single statistical feature is relatively poor. Camera noise shows the best effect among the three features. Therefore, it is effective to focus on camera noise as the main feature of this paper. From the results, we can see that the final accuracy of the classifier training for the extraction of composite features in this paper is about 97.4%, which has greatly improved compared with single texture and statistical features.

In order to evaluate the effectiveness of the composite features based on the three types of features proposed in this paper, this article conducted experiments on different data sets, namely MICC-F200, MICC-F2000 and CASIA 2.0. The specific experimental results are shown in Table. 3 below.

TABLE 3. Performance of the proposed method

Dataset	Precision (%)	Recall (%)	F1 score(%)	Accuracy (%)
MICC-F220	90.00	99.08	94.32	94.06
MICC-F2000	91.44	96.14	93.73	95.50
CASIA 2.0	98.22	96.94	96.19	97.40

It can be concluded from the table that the composite features show better performance on these data sets. Therefore, feature selection based on the inconsistency of the three characteristics is effective. In addition, in order to verify the effectiveness of the composite feature relative to a single feature, a single feature experiment was also performed on each data set. Here, a line graph is used to represent it, as shown in the figure below. The following line graph shows the performance of the algorithm in this paper on four data sets and the individual performance of the three types of features. Among them, the green line represents the composite feature. It can be seen from the four pictures that the composite feature can achieve a higher detection effect compared to the three types of individual features.

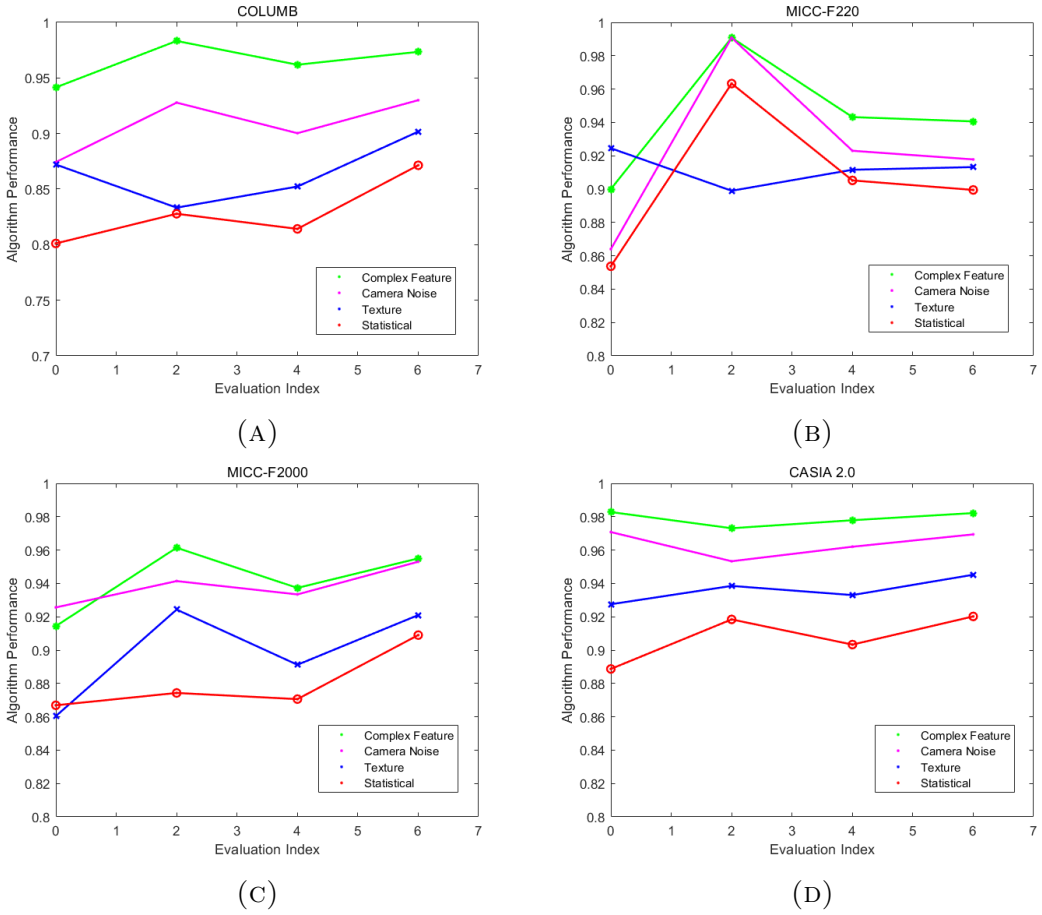

FIGURE 4. Algorithm performance on different data sets.

4. **Conclusion and Future Works.** This paper mainly proposes an image splicing tampering detection method based on the composite features of camera, texture and statistics. After tampering, the consistency of content features such as histograms, high-order statistics, or texture features will be destroyed. By selecting the camera noise characteristics of the three channels, the accuracy of the detection can be improved. In this paper, the identification of natural images and spliced images is carried out in the form of composite features, and the identification effect has been greatly improved. Since this paper uses a variety of feature fusion, the experiment evaluates and compares the performance of single feature and composite feature. Although the accuracy results have been significantly improved, the accuracy is still not ideal. It may be because the above-mentioned features cannot fully describe the essential features of the image, so future improvement work can start from the selection of image features. We can find a more accurate method to improve the accuracy of image representation, and we can study and extract more effective features, such as fractal dimension, CFA interpolation, etc. As we all know, image interpolation has an important influence on various characteristics of natural images. Therefore, we can study these features in depth and find the essential features of natural images.

Acknowledgment. This work is partially supported by Science Foundation of Zhejiang Sci-Tech University(ZSTU) under Grant No.19032458-Y. The authors also gratefully acknowledge the helpful comments and suggestions of the reviewers, which have improved the presentation.

REFERENCES

[1] J. Lukáš, J. Fridrich, and M. Goljan, "Detecting digital image forgeries using sensor pattern noise," *Proceedings of SPIE - The International Society for Optical Engineering*, pp.362–372, 2006.

[2] M. Goljan, J. Fridrich, F. Toma, "Large scale test of sensor fingerprint camera identification, media forensics and security," *International Society for Optics and Photonics*, vol.7254, pp.72540, 2009.

[3] E. D. Iii, M. Goljan, and J. Fridrich, (eds.), "Camera identification from cropped and scaled images," *International Society for Optics and Photonics*, no.68190E, 2008.

[4] M. Goljan, J. Fridrich, and C. Mo, "Sensor noise camera identification: countering counter-forensics," *Media Forensics and Security II, part of the IS&T-SPIE Electronic Imaging Symposium*, San Jose, CA, USA, vol. 7541, pp. 18-20, 2010.

[5] M. Goljan, J. Fridrich, and C. Mo, "Defending against fingerprint-copy attack in sensor-based camera identification," *IEEE Transactions on Information Forensics & Security*, vol. 6, No. 1, pp. 227-236, 2011.

[6] M. Goljan, J. Fridrich, and T. Filler, "Managing a large database of camera fingerprints," *2019 Proceedings of SPIE - The International Society for Optical Engineering*, vol. 7541, no. 3, pp. 175-178, 2010.

[7] N. D. Memon, J. Fridrich, and M. Goljan, (eds.), "Determining approximate age of digital images using sensor defects," *2019 Proceedings of SPIE - The International Society for Optical Engineering*, vol.7880, pp. 06-11, 2011.

[8] M. Goljan, J. Fridrich, "Sensor-fingerprint based identification of images corrected for lens distortion," *Proceedings of SPIE - The International Society for Optical Engineering*, vol. 8303, no. 12, 2012.

[9] G. Chierchia, S. Parrilli, and G. Poggi, (eds.), "On the influence of denoising in PRNU based forgery detection," *2nd ACM workshop on Multimedia in Forensics Security and Intelligence*, pp. 117-122, 2010.

[10] G. Chierchia, G. Poggi, and C. Sansone, (eds.), "PRNU-based forgery detection with regularity constraints and global optimization," *2013 IEEE 15th International Workshop on Multimedia Signal Processing (MMSP)* IEEE, 2013.

[11] X. Pan, X. Zhang, S. Lyu, "Exposing image splicing with inconsistent local noise variances," *2012 IEEE International Conference on Computational Photography (ICCP)*, pp. 1-10, 2012.

[12] C. M. Pun, B. Liu, and X. C. Yuan, "Multi-scale noise estimation for image splicing forgery detection," *Journal of Visual Communication & Image Representation*, vol. 38, no.6, pp. 195-206, 2016.

[13] D. Cozzolino, D. Gragnaniello and L. Verdoliva, "Image forgery localization through the fusion of camera-based, feature-based and pixel-based techniques," *2020 2014 IEEE International Conference on Image Processing (ICIP)*, pp. 5302-5306, 2014.

[14] L. Gaborini, P. Bestagini, and S. Milani, (eds.), "Multi-clue image tampering localization," *2014 IEEE International Workshop on Information Forensics and Security (WIFS)*, pp. 125-130, 2014.

[15] A. T. P. Ho, F. Retraint, "Effective images splicing detection based on decision fusion," *2019 IEEE International Symposium on Signal Processing and Information Technology (ISSPIT)*, pp. 1-5, 2019.

[16] X. Tang, W. Zhang, and Y. Chen, "Image tampering localization based on superpixel segmentation," *2020 International Conferences on Internet of Things (iThings)*, Rhodes, Greece, pp. 597-602, 2020.

[17] X. Lin, C. T. Li, "PRNU-based content forgery localization augmented with image segmentation," *IEEE Access*, vol. 8, pp. 222645-222659, 2020.

[18] D. Cozzolino, L. Verdoliva, "Noiseprint: a CNN-based camera model fingerprint," *IEEE Transactions on Information Forensics and Security*, vol. 15, pp. 144-159, 2020.

[19] E. K. Wang, C. M. Chen and M. M. Hassan, (eds.), "A deep learning based medical image segmentation technique in internet-of-medical-things domain," *Future Generation Computer Systems*, vol. 108, 2020.

[20] K. Wang, C. M. Chen, M. S. Hossain, (eds.), "Transfer reinforcement learning-based road object detection in next generation IoT domain," *Computer Networks*, vol. 193, 2021.

[21] S. Kumar, A. Damaraju, A. Kumar, (eds.), "LSTM network for transportation mode detection," *Journal of Internet Technology*, vol. 22, no. 4, pp. 891-902, 2021.